Authors’ Response to Reviews of

“Insoluble lipid film mediates the transfer of soluble saccharides from the sea to the atmosphere: the role of hydrogen bonding”

Minglan Xu, Narcisse Tsona Tchinda, Jianlong Li, Lin Du*

We thank the Referee for the constructive comments. We have addressed the comments point by point below and modified the manuscript accordingly. For clarity, the Referee’s comments (RC) are reproduced in blue, authors’ responses (AR) are in black and changes in the manuscript are in red color text.

Referee #2

This manuscript presents an important contribution to the understanding of saccharide transfer and enrichment in sea spray aerosol. The authors conduct a thorough experimental investigation in which both particle properties and fundamental physicochemical properties of the air/water interface are investigated. The molecules used within this study represent important and abundant contributors to sea spray aerosol composition, and the composition was carefully selected to serve as a good model system. Additionally, the manuscript is well-written, and the results are summarized clearly and succinctly. While I think that the main arguments presented in the manuscript are reasonable, I believe that several clarifying details and/or a few additional control experiments will make the conclusions more convincing.

RC: What was the pH of the seawater solution at the beginning and end of the experiments? Basic solutions acidify over time when exposed to air due to atmospheric carbon dioxide, and pH changes can dramatically change the film morphology and saccharide adsorption to the monolayer. Carter-Fenk and Allen (Carter-Fenk, K. A.; Allen, H. C. Collapse Mechanisms of Nascent and Aged Sea Spray Aerosol Proxy Films. Atmosphere **2018**, 9 (12), 503. https://doi.org/10.3390/atmos9120503.) demonstrate these pH-dependent changes using the same proxy monolayer mixture, 2 MA : 4 PA : 3 SA. The film morphology and isotherm change as a function of pH, and the myristic acid solubility decreases with decreasing pH. Consequently, any solution acidification could enhance myristic acid adsorption to the air/water interface, thereby expanding the monolayer and increasing the observed mean molecular area in the surface pressure-area isotherms. Carter-Fenk et al. also show how the subphase pH impacts saccharide co-adsorption to a palmitic acid and cetyl alcohol monolayer, albeit using different saccharides (Carter-Fenk, K. A.; Dommer, A. C.; Fiamingo, M. E.; Kim, J.; Amaro, R.; Allen, H. C. Calcium Bridging Drives Polysaccharide Co-Adsorption to a Proxy Sea Surface Microlayer. Phys. Chem. Chem. Phys. **2021**, 23 (30), 16401–16416. https://doi.org/10.1039/D1CP01407B). The fatty acid carboxylic acid protonation state can change near seawater pH, and the overall monolayer protonation state impacts the intermolecular interactions between saccharides and monolayer headgroups at the air/water interface. For further discussion on the surface pKa of fatty acids at the air/water interface, see the following references: Wellen, B. A.; Lach, E. A.; Allen, H. C. Surface pKa of Octanoic, Nonanoic, and Decanoic Fatty Acids at the Air–Water Interface: Applications to Atmospheric Aerosol Chemistry. Phys. Chem. Chem. Phys. **2017**, 19 (39), 26551–26558. https://doi.org/10.1039/C7CP04527A.; Zhang, T.; Brantley, S. L.; Verreault, D.; Dhankani, R.; Corcelli, S. A.; Allen, H. C. Effect of pH and Salt on Surface pKa of Phosphatidic Acid Monolayers. Langmuir **2018**, 34 (1), 530–539. https://doi.org/10.1021/acs.langmuir.7b03579.

AR: As the Referee said, the strong change in pH from basic to neutral and acidic does have a great effect on the film morphology and π-A isotherm. The proxy monolayer mixture (2 MA: 4 PA: 3 SA) was spread on NaCl subphase at pH 8.2, 5.6 and 2.0 to simulate the composition of SSA aqueous cores from nascent to aging in the marine boundary layer (Carter-Fenk and Allen, 2018). At pH 8.2, the SSA proxy monolayer undergoes a two-dimensional phase transition from a gaseous-tilted condensed (G-TC) coexisting phase to a tilted condensed (TC) phase at 24 Å^2/molecule (lift-off area). After further compression of the TC phase, the monolayer transitioned to the untitled condensed (UC) phase at a surface pressure of 18 mN/m. The maximum surface pressure of the film is around 70 mN/m. At pH 5.6, the lift-off point of monolayer occurs at 25 Å^2/molecule, and a surface pressure plateau at collapse occurs at ~64 mN/m. The collapse pressure on 0.4 M NaCl at pH 5.6 is slightly lower than that at pH 8.2. When the SSA proxy film is completely protonated on 0.4 M NaCl at pH 2.0, the lift-off area is significantly higher at 28 Å^2/molecule, and the π-A isotherm reaches a maximum surface pressure of ~ 58 mN/m before the surface pressure decreases. Combined with Brewster angle microscope (BAM) to visualize the SSA proxy collapse structure, the results showed that at nascent SSA pH, the mixture produced a monolayer with moderate rigidity, which folded when the film was compressed to a collapsed state. However, acidification makes the SSA proxy film to become more rigid and form three-dimensional (3D) nuclei.

In addition, the pH change of the solution also changes the protonation state of the carboxylic acid. Recent work by Carter-Fenk et al. has shown the alginate (a linear anionic polysaccharide) co-adsorption to d_{31}-palmitic acid monolayers, and investigated the effects of different pH values (Carter-Fenk et al., 2021). The carboxylic acid protonation state was varied through the solution pH values of 8.2 and 5.8. Palmitic acid has a reported surface pKa between 8.34 and 8.7, and the pKa values of alginate G and M residues are 3.7 and 3.4, respectively. Thus at seawater pH of 8.2, palmitic acid is partially deprotonated and alginate is fully deprotonated. At pH 5.8, palmitic acid is mostly protonated, and alginate carboxylate groups remain deprotonated. It was found that the protonation state of palmitic acid significantly affected the degree of alginate co-adsorption. For the d_{31}-palmitic acid monolayer at pH 5.8, alginate co-adsorption degree decreased compared with the chemical system at pH 8.2. Therefore, increased d_{31}-palmitic acid protonation decreases the extent of alginate co-adsorption.

In our study, we measured the pH of the seawater solution before and after the experiments. The results showed that the natural seawater used had a pH of approximately 8.13±0.02, which was measured at about 8.04±0.01 after exposure to air in the Langmuir trough for about 2 h during the experiment period. That is to say, no matter in the experiment of measuring π-A isotherm or infrared reflection-absorption spectra, the change in pH value of seawater remains at about 0.1, and the overall acidification is relatively slow. Minor changes in pH therefore do not have very strong effects on protonation and deprotonation state of fatty acids. Therefore, we infer that the effect on the π-A isotherm and IRRAS spectral measurements due to changes in seawater pH should not be the dominant factor during the experiment. We have explained the pH changes throughout the experiment in the revised manuscript at page 8:

The pH of natural seawater, initially determined to be about 8.13±0.02, was measured to be around 8.04±0.01 at the end of the experiment.

RC: The partial dissolution of myristic acid most likely accounts for the smaller mean molecular area observed in the proxy mixture isotherm compared to the palmitic acid and stearic acid isotherms (Figure 3). Myristic acid increases the fluidity of the monolayer, thereby expanding the surface pressure-area isotherm when myristic acid remains adsorbed to the surface (see https://doi.org/10.3390/atmos9120503 for further discussion).

AR: In this study, myristic acid (MA) was the shortest of the selected long-chain fatty acids, and the sum of the dispersion interactions produced between the lipids was small. Therefore, the MA film at the air-water interface is more disordered and less tightly packed (Gericke and Huhnerfuss, 1993). The MA is partially soluble in water (Patil et al., 1973), and due to the strong electrostatic interaction between the carboxylate moiety and the water molecules, the desorption rate of MA increases with the deprotonation of the carboxylic acid headgroups. At 20 °C, according to the surface pKa value of 7.88 (Mclean et al., 2005), MA is mostly deprotonated at pH ~8.1, so a stable monolayer cannot be obtained for the natural seawater subphase due to the dissolution phenomenon. In the π−A isotherm experiment, the mechanical forcing from lateral barriers compression also promotes desorption. Therefore, the MA monolayer is unstable and cannot reach collapse. It could also help explain why the π-A isotherm of proxy monolayer mixture occupied a smaller mean molecular area. The partial dissolution of myristic acid may play a role. We have made a further discussion for this phenomenon in the revised manuscript at page 19:

The partial dissolution of myristic acid most likely accounts for the smaller mean molecular area observed in the proxy mixture isotherm compared to the palmitic acid and stearic acid isotherms.

RC: In line 325, the authors mention a “kink point” in the palmitic acid isotherm at ~40 mN/m. Palmitic acid should not have a phase transition at this point. It is possible that this “kink point” is caused by a contaminant that is being squeezed out upon monolayer compression. Does the “kink point” remain upon using a new palmitic acid and chloroform solution? Does the “kink point” disappear when compressing the barriers at 5 mm/min/barrier instead of 3 mm/min?

AR: Before each measurement of the π-A isotherm, we thoroughly cleaned the trough and barriers with reagent alcohol and ultrapure water to ensure contamination-free. Moreover, if the contamination was due to palmitic acid stock solution, the π-A isotherm of the mixed fatty acid would also show a similar turning point near this surface pressure. For mixed fatty acids, however, there was no such twist. Therefore, we can basically rule out the contamination caused by palmitic acid stock solution. Although we cannot clearly explain the reasons for this phenomenon at that time, the π-A isotherm was re-determined using freshly prepared palmitic acid solution and the results are shown in Figure 3 in the revised manuscript. For the π-A isotherm of the newly determined palmitic acid, we found that its π-A isotherm with stearic acid and mixed fatty acids does exhibit similar collapse behavior at a surface pressure of about 50 mN/m. We have revisited this section in the revised manuscript at page 18-19:

After experiencing a kink point at ~48 mN m^{-1}, it continues to rise to the maximum surface pressure of ~57 mN m^{-1} and collapses. Both the lift-off area and molecular area of the stearic acid film decreased more than those of palmitic acid film. This is caused by the fact that the interaction (van der Waals force) between the molecules increases as the molecular weight of long chain fatty acid increases. That is, increased attraction leads to a decrease in distance between SA molecules.

The partial dissolution of myristic acid most likely accounts for the smaller mean molecular area observed in the proxy mixture isotherm compared to the palmitic acid and stearic acid isotherms. Moreover, we found that the π-A isotherms of mixed fatty acids exhibit similar collapsing behavior to those of stearic acid and palmitic acid at a surface pressure of about 50 mN m^{-1}.

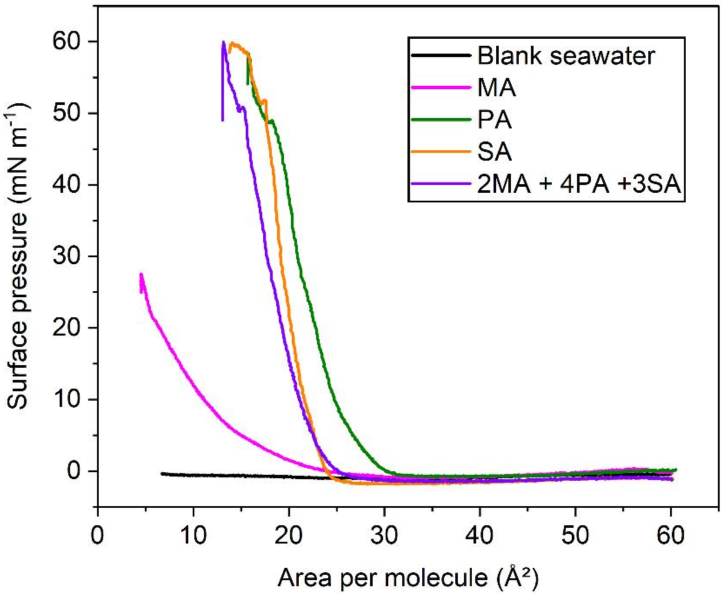

Figure 3. π-A isotherms of myristic acid, palmitic acid, stearic acid and mixed fatty acids. The black trace represents the background natural seawater solution with no fatty acid spread.

Regarding the barrier compressing speed, the 3 mm/min we chose for this study was determined based on our previous pre-experimental results. We have used stearic acid film as an example to investigate the effect of barrier moving speed on its π-A isotherms. When the amount of organic solution was 50 μL and the volatilization time was 15 min, the two barriers compressed the stearic acid molecules at a uniform speed of 1, 3, and 6 mm/min to obtain π-A isotherms of their monolayers. It was found that the isotherms obtained at 1 and 3 mm/min were very close, and when the barrier compressing speed reached 6 mm/min, the entire isotherm shifted to the right. When the barrier compressing rate is slow enough, it can be assumed that the film is in equilibrium state, while the surface pressure value obtained in the non-equilibrium state is obtained when compressed quickly. Therefore, a barrier moving speed of 3 mm/min is appropriate for this study.

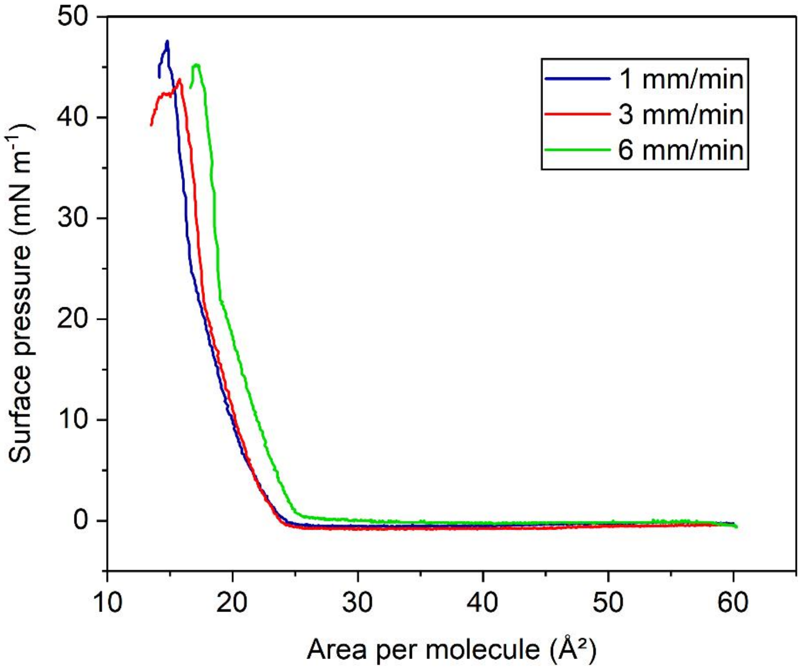

Figure R1. The influence of barrier moving speed on π-A isotherms of stearic acid monolayer.

RC: In line 206, the barrier compression speed should be specified as 3 mm/min/barrier (if that is the case).

AR: Thanks for the Referee's reminder. We have modified it in the revised manuscript at page 11:

> The barriers were compressed at a rate of 3 mm min^{-1} per barrier and isotherm data were collected for surface pressure π (mN m^{-1}) versus area per molecule (Å^2).

RC: In lines 353-355, the authors cite Vazquez de Vasquez et al., 2022 (https://doi.org/10.1021/acsearthspacechem.2c00066) for saccharide concentrations in the ocean. The authors should instead cite the original papers for these measurements: https://doi.org/10.1016/0304-4203(92)90020-B, https://doi.org/10.1021/cr500713g, and https://doi.org/10.1021/acsearthspacechem.9b00197. However, Vazquez de Vasquez et al. corroborate the authors' argument that the saccharides interact with the monolayer headgroups and expand the monolayer. Additionally, Vazquez de Vasquez et al. argue that glucuronate intercalates into a stearic acid monolayer. Thus, a brief discussion and/or statement on the Vazquez de Vasquez et al. results is warranted in the context of this manuscript's conclusions on the saccharide-carboxylic acid hydrogen bonding interactions. This statement/discussion would perhaps fit in with the discussion in lines 368-375.

AR: We have cited the original literature recommended by the Referee in the revised manuscript at page 20:

> Considering that saccharides in the ocean represent approximately 20% of the dissolved organic carbon (Pakulski and Benner, 1992; Hasenecz et al., 2019), the saccharide concentration is about 0.14–0.20 mg L^{-1}.

Vazquez de Vasquez et al. investigated the co-absorption of alginate and its representative monomeric form glucuronate to a stearic acid monolayer as a function of saccharide concentration on an ocean proxy solution (De Vasquez et al., 2022). Their experimental results showed that for glucuronate, the film reached a maximum surface pressure in the range ~ 60–65 mN/m, while the mixed proxy film reached a maximum surface pressure between 50 mN/m and 60 mN/m in our experiments. In the case of glucuronate, they also observed that the monolayer expansion is not monotonic. The drastic expansion, or an increase in the surface area of individual molecules increases disproportionately, which strongly indicates that it exists at the interface where it destroys the packing of the monolayer. However, no such disproportionality was observed for the two saccharides we studied. As the concentration of glucuronate increases, small changes in the brightness of the BAM image also point to the glucuronate intercalation into the monolayer, producing reorganization. Using Langmuir isotherms, surface-sensitive infrared reflection-absorption spectroscopy and Brewster angle microscopy, they demonstrate that glucuronate may intercalate and induce significant reorganization within the monolayer. Data on glucuronate co-adsorption to the deprotonated monolayer suggest that glucuronate surface propensity is a contributor to saccharide composition. The results of Vazquez de Vasquez et al. have been further discussed in a comparative way in the revised manuscript at page 21-22:

> De Vasquez et al. (2022) also demonstrated that glucuronate interacts with and expands the stearic acid monolayer. Furthermore, they suggested that glucuronate intercalates into the stearic acid monolayer and leads to monolayer reorganization. Spectral evidence is needed to further clarify whether intercalation occurs in our study.

RC: Lines 380-383: Due to the partial solubility of myristic acid at seawater pH, it is possible that higher concentrations of glucose or trehalose simply decrease the myristic acid solubility due to competitive hydration. In other words, the saccharides are weakly “salting out” the myristic acid from the seawater, enhancing myristic acid adsorption at the air/water interface and expanding the monolayer. I recommend conducting a control experiment in which the surface pressure of myristic acid alone is monitored as a function of saccharide concentration. Spread the same amount of myristic acid on the seawater surface, and test whether higher concentrations of saccharides increase the surface pressure (increase myristic acid adsorption). Normalize the change in surface pressure to any changes in the subphase surface tension due to the different concentrations of saccharides in the seawater. Alternatively, the authors could use deuterated myristic acid and track the C-D vibrational modes with IRRAS as a function of saccharide concentration. If the overall intensity of the C-D modes do not change with increasing saccharide concentration, then the saccharides are not impacting myristic acid adsorption at the air/water interface.

AR: As the Referee noted, high concentrations of glucose or trehalose do have the potential to “salt out” myristic acid weakly from seawater and reduce its solubility. Therefore, the adsorption of myristic acid at the air/water interface was enhanced and the monolayer was expanded. According to the Referee’s suggestion, we supplemented a set of controlled experiments in which the surface pressure of myristic acid alone is monitored as a function of the same saccharide concentration. As shown in Figure R2, we found that high concentrations of glucose do not increase the surface pressure, but all manifest as a decrease in surface pressure. In particular, the decrease in surface pressure is most significant when the maximum concentration of glucose is 5 g L^{-1}. Therefore, enhanced surface adsorption of myristic acid due to salting out may not have played an important role in this study.

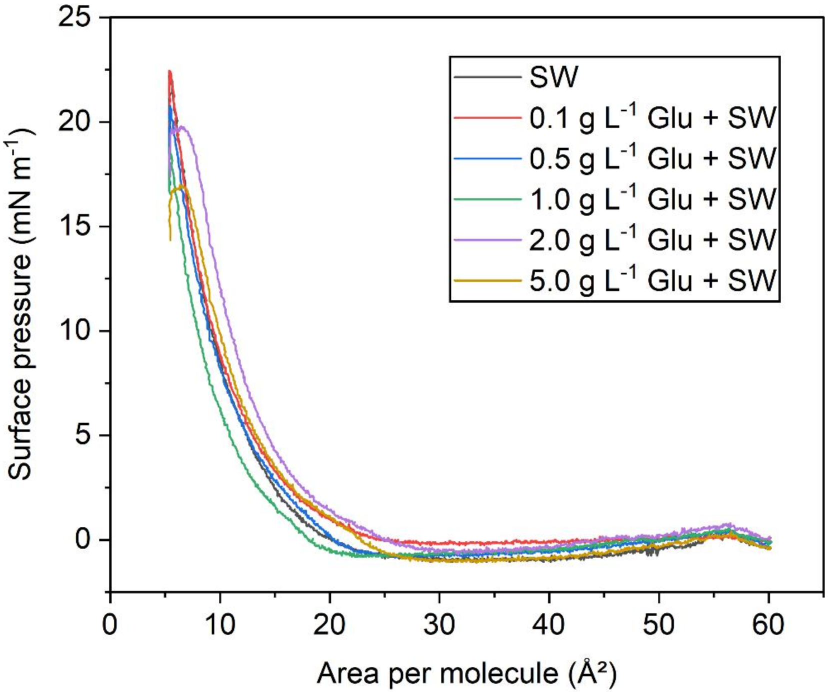

Figure R2. π-A isotherms of myristic acid in the SW subphase with several concentration gradients of glucose.

RC: Lines 386-389: Another change in isotherm slope, or “kink point”, is observed in the proxy monolayer mixtures with saccharides. Is it possible that this change in slope is due to the same “kink point” observed in the palmitic acid isotherm (especially due to the large mole fraction of palmitic acid within the mixture)? Was the same palmitic acid sample used in the preparation of the proxy mixture? Is it possible that some contaminant is making its way into both the palmitic acid + chloroform solution and the proxy mixture + chloroform solutions?

AR: To maintain the uniformity of experimental results, we used the same prepared palmitic acid-chloroform solution and proxy mixture-chloroform solution. Additionally, not all isotherms have such a turning point, so we speculate that contamination may not cause the kink point to be created under this surface. Therefore, it may be caused by other reasons that are not yet clear.

RC: The sentence in lines 456-457 (“This band component is put down to the conformation with the carbonyl group almost parallel to the water surface.”) is unclear.

AR: IRRAS spectroscopy not only can characterize the order of hydrophobic alkyl chain packing, but also provide information on the interactions between monolayer and seawater subphase through the determination of hydrophilic groups. It mainly includes carbonyl stretching vibration modes (ν(C=O)), carboxylate asymmetric (ν_{as}(COO)) and symmetric (ν_{s}(COO)) stretching vibration modes. In Figure 6, multiple stretching vibration modes of the carbonyl group can be observed near 1734, 1725 and 1708 cm^{-1}. These three characteristic peaks are known to correspond to unhydrogen bonded, the singly and doubly hydrogen bonded carbonyl group in a saturated fatty acid. This is due to the formation of hydrogen bonds between them and water subphase or adjacent fatty acid molecules will cause the red shift of the ν(C=O). In addition, according to the spectra, it can be found that for different components of subphase, the relative strength of the three bands is different.

Of note is that the conformation of the carboxylic group to the water depends on the conformation of the hydrocarbon chain. According to the different alkyl chain and headgroup configurations, fatty acid molecules can be divided into four types (I, I’, II and III) as shown in Figure R3 (Muro et al., 2010). In types I and I’, fatty acid molecules are arranged in an orderly tilted straight chain structure, where the C=O and O−H groups rotate around α carbon to form *cis* and *trans* conformations. The O−H group is oriented toward the water phase in the *cis* conformation and away from water in the *trans* conformation. In comparison, the former (type I) would be favored by hydration, while the *trans* conformation (type I’) is not suitable for hydration. Different from types I and I’, the alkyl chain in type II is a disordered *gauche* conformation near the headgroup, resulting in the carboxylic acid headgroup entering the subphase as a whole, and the rotation of the headgroup does not affect the formation of hydrogen bonds. In addition to forming hydrogen bonds with water subphase, hydrogen bond networks (type III) can also be formed when the molecules of type II are closely packed with each other. Among these conformations, only C=O of type I is retained in the gas phase, which is not conducive to the formation of hydrogen bond between type I and water subphase, thus forming the characteristic peak around 1734 cm^{-1}. The fatty acid molecules in type III form a hydrogen bond network and then further hydrate with the subphase, and the monolayer under the action of this strong hydrogen bond is the most stable, forming the characteristic peak with the lowest wavenumber (~1708 cm^{-1}). Then, the band at 1725 cm^{-1} is assigned to type II that is hydrated but not involved in the hydrogen bonding network.

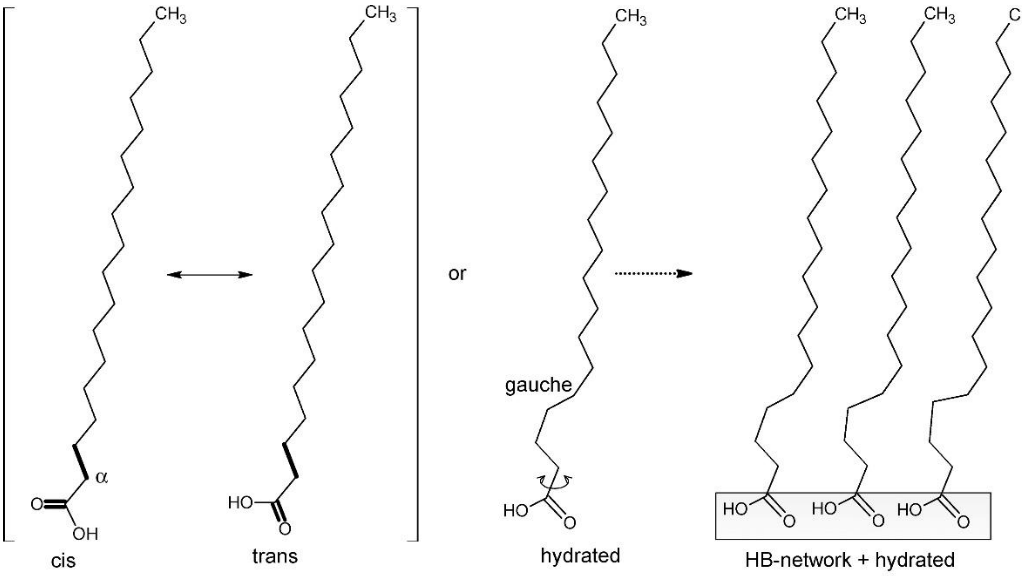

(a) Type I (b) Type I' (minor) (c) Type II (d) Type III

Figure R3. Molecular schemes of a fatty acid with different conformations of the carboxylic group and different conformations of the hydrocarbon chain.

We have rewritten this sentence to make it clear and easy to understand in the revised manuscript at page 25:

This band component at 1734 cm^{-1} is put down to the conformation with the carbonyl group almost parallel to the water surface and the hydroxyl group is oriented toward the water surface, which is not conducive to the formation of hydrogen bond with water subphase (Muro et al., 2010).

RC: How are the center frequencies of the IRRAS peaks being determined? Are the peaks being fitted to Gaussian functions? It would be helpful to have a table (perhaps in the Supplement) of the carbonyl peak center frequencies at the various saccharide concentrations to more readily understand how the vibrational frequencies are changing.

AR: We collected the IRRAS spectra with 2000 scans and a resolution of 8 cm^{-1}, so a better signal-to-noise ratio can be obtained. The displayed infrared spectra can basically distinguish the frequency of each peak well. However, in order to make better identification, we also carried out Gaussian fitting based on the measured

IRRAS spectra, and redrew the infrared spectra to display in the revised manuscript. In addition, we also added a table in the supplement to summarize the wavenumbers, reflectance-absorbance intensities, peak areas and full width at half maximum (FWHM, cm^{-1}) values of each fitted peak.

The carbonyl stretching modes (ν(C=O)) of the carboxyl group at ~1734 cm^{-1} (unhydrogen bonded), 1725 cm^{-1} (singly hydrogen bonded) and 1708 cm^{-1} (doubly hydrogen bonded) were observed in seawater (Gericke and Huhnerfuss, 1993), with the strength at 1734 cm^{-1} being the highest (Figure 6). This band component at 1734 cm^{-1} is put down to the conformation with the carbonyl group almost parallel to the water surface and the hydroxyl group is oriented toward the water surface, which is not conducive to the formation of hydrogen bond with water subphase (Muro et al., 2010). For saccharide concentrations ranging from 0.1 to 2 g L^{-1}, the unhydrated C=O band was observed to be depressed, and the singly and doubly hydrogen bonded carbonyl components at ~1720 and ~1708 cm^{-1} became dominant (Johann et al., 2001). At the highest glucose concentration, the Langmuir model appears to capture a saturation effect, where the establishment of hydrogen bonds is associated with a strong initial increase in glucose organic enrichment, followed by surface saturation at higher organic concentration. We also displayed the wavenumbers, reflectance-absorbance intensities, peak areas and full width at half maximum (FWHM, cm^{-1}) values of each fitted peak in the region of 1800–1300 cm^{-1} in Table S3 in the supplement.

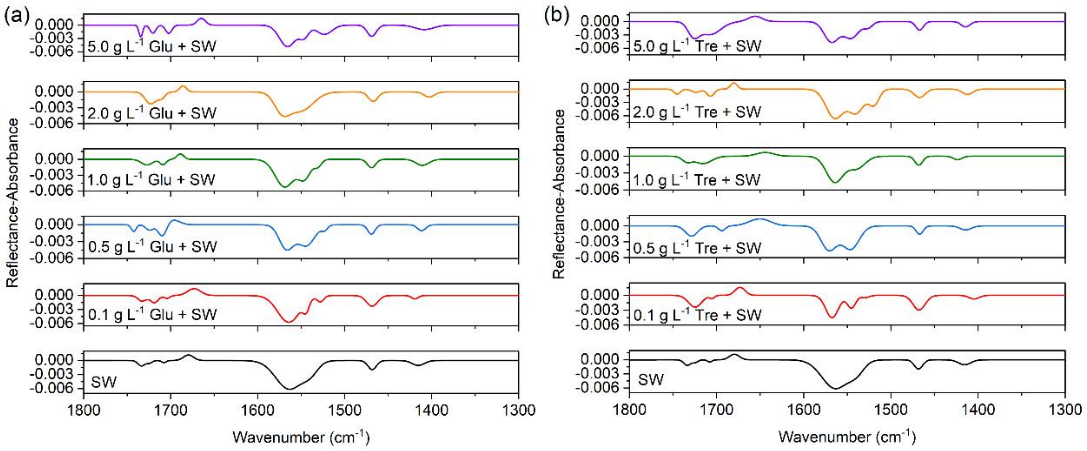

Figure 6. PM-IRRAS spectra (1800–1300 cm^{-1}) of mixed fatty acids at the air/seawater interface at different (a) glucose, and (b) trehalose concentrations in the subphase.

RC: The sentence in lines 465-467 states: “We believe that saccharides displace water surrounding the fatty acid polar headgroups and interact strongly with both water and lipid headgroups, resulting in a slight increase in hydration near the monolayer interface.” Shouldn’t saccharide adsorption decrease hydration near the monolayer interface due to saccharides displacing water to interact with the monolayer headgroups?

AR: We have made the modification in the revised manuscript at page 26:

> We believe that saccharides displace water surrounding the fatty acid polar headgroups and interact strongly with lipid headgroups, resulting in a slight decrease in hydration near the monolayer interface.

RC: Lines 487-488: Again, how were the center frequencies determined for the carboxylate stretching modes? Are there three peaks if individual spectra are decomposed into Gaussians? Secondly, the shifts to higher frequencies in the carboxylate stretching modes might be indicative of carboxylate dehydration upon interactions with saccharides.

AR: We performed Gaussian fitting within the COOH stretching region (1800-1300 cm^{-1}), and redrew the infrared spectra to display in the revised manuscript. In addition, we also added a table in the supplement to summarize the wavenumbers, reflectance-absorbance intensities, peak areas and full width at half maximum (FWHM, cm^{-1}) values of each fitted peak.

Indeed, we found a shift in the carboxylate stretching mode to higher frequencies, which may be a hallmark of carboxylate dehydration upon interactions with saccharides. We have expanded this discussion in the revised manuscript at page 28:

> The broad and strong antisymmetric carboxylate stretch (ν_{as}(COO)) were observed at ~1564 cm^{-1}, and the symmetric carboxylate stretch (ν_{s}(COO)) at ~1415 cm^{-1}. The presence of salt in seawater caused the ν_{as}(COO) to split into three peaks at ~1564, ~1544 and ~1528 cm^{-1}. Additionally, we found a shift in the major carboxylate stretching mode from 1564 to higher frequency ~1572 cm^{-1}, which may be indicative of carboxylate dehydration upon interactions with saccharides.

References

Carter-Fenk, K. A. and Allen, H. C.: Collapse mechanisms of nascent and aged sea spray aerosol proxy films, Atmosphere, 9, 503, ARTN 503 10.3390/atmos9120503, 2018.
Carter-Fenk, K. A., Dommer, A. C., Fiamingo, M. E., Kim, J., Amaro, R. E., and Allen, H. C.: Calcium bridging drives polysaccharide co-adsorption to a proxy sea surface microlayer, Phys. Chem. Chem. Phys., 23, 16401-16416, 10.1039/d1cp01407b, 2021.
de Vasquez, M. G. V., Rogers, M. M., Carter-Fenk, K. A., and Allen, H. C.:

Discerning poly- and monosaccharide enrichment mechanisms: Alginate and glucuronate adsorption to a stearic acid sea surface microlayer, ACS Earth Space Chem., 6, 1581-1595, 10.1021/acsearthspacechem.2c00066, 2022.

Gericke, A. and Huhnerfuss, H.: In-situ investigation of saturated long-chain fatty-acids at the air-water interface by external Infrared reflection-absorption spectrometry, J. Phys. Chem., 97, 12899-12908, 10.1021/j100151a044, 1993.

McLean, D. S., Vercoe, D., Stack, K. R., and Richardson, D.: The colloidal pKa of lipophilic extractives commonly found in Pinus radiata, Appita J. J. Tech. Assoc. Aust. N. Z. Pulp Pap. Ind., 58, 362-366, 10.3316/informit.582876014112177, 2005.

Muro, M., Itoh, Y., and Hasegawa, T.: A conformation and orientation model of the carboxylic group of fatty acids dependent on chain length in a Langmuir monolayer film studied by polarization-modulation infrared reflection absorption spectroscopy, J. Phys. Chem. B, 114, 11496-11501, 10.1021/jp105862q, 2010.

Patil, G. S., Matthews, R. H., and Cornwell, D. G.: Kinetics of processes of desorption from fatty-acid monolayers, J. Lipid Res., 14, 26-31, 10.1016/S0022-2275(20)39325-1, 1973.